

Influence of Topological Excitations on Shapiro Steps and Microwave Dynamical Conductance in Bilayer Exciton Condensates

Timo Hyart and Bernd Rosenow

Institut für Theoretische Physik, Universität Leipzig, D-04103 Leipzig, Germany

(Received 7 August 2012; published 15 February 2013)

The quantum Hall state at total filling factor $\nu_T = 1$ in bilayer systems realizes an exciton condensate and exhibits a zero-bias tunneling anomaly, similar to the Josephson effect in the presence of fluctuations. In contrast to conventional Josephson junctions, no Fraunhofer diffraction pattern has been observed, due to disorder induced topological defects, so-called merons. We consider interlayer tunneling in the presence of microwave radiation, and predict Shapiro steps in the tunneling current-voltage characteristic despite the presence of merons. Moreover, the Josephson oscillations can also be observed as resonant features in the microwave dynamical conductance.

DOI: [10.1103/PhysRevLett.110.076806](https://doi.org/10.1103/PhysRevLett.110.076806)

PACS numbers: 73.43.Jn, 03.75.Lm, 67.10.-j

Quantum Hall (QH) systems are an ideal platform to study the rich diversity of exotic effects induced by Coulomb interactions [1,2]. One state of particular interest is an exciton condensate occurring in QH bilayers at the total filling factor $\nu_T = 1/2 + 1/2 = 1$ [1–24]. Recently, there has been growing interest in similar exciton condensate states in bilayer graphene [25,26] and topological insulator thin films [27], and in this Letter the QH bilayer state serves as a prototype system for exciton condensates with interesting topological excitations. Although the excitons are charge neutral, the bilayer nature of these states allows remarkable electronic properties such as almost dissipationless counterflow currents, strong enhancement of the tunneling conductance due to the Josephson effect, and a quantized Hall drag resistance [1–13], which have been observed experimentally [14–24].

The macroscopic phase coherence in Josephson junctions (JJs) was originally confirmed by measuring the dependence of the tunneling current on magnetic field [28] and microwave radiation [29]. In the first type of experiment, oscillations of the critical current were observed as a function of the magnetic flux Φ applied across the junction. Because of the spatial coherence of the superconductors, the tunneling current vanishes for an integer number of superconducting flux quanta $h/2e$ in the junction, in analogy to the Fraunhofer diffraction pattern of light. On the other hand, the application of microwave radiation allows the observation of the ac Josephson effect. Namely, when the phase difference between the two superconductors oscillates both at the Josephson frequency $2eV_{\text{dc}}/\hbar$ determined by the dc voltage and at the microwave frequency ω , steps arise in the current-voltage (I - V) characteristic whenever $2eV_{\text{dc}} = n\hbar\omega$ ($n = 0, 1, 2, \dots$). In this Letter, we show that in QH bilayers the Fraunhofer pattern is typically not observable due to a spatial randomization of the phase, but Shapiro steps are still expected when the correlation time is longer than the microwave period. Shapiro steps are more robust because they test

extended correlations in time but do not depend on a spatial regularity of the condensate phase.

In QH exciton condensates, a weak tunnel coupling between the layers gives rise to Josephson-like effects [6], with the Cooper pair charge $2e$ replaced by the electron charge e . However, the QH exciton condensate supports exotic topological excitations, so-called merons. They are vortices of the order parameter field and carry a charge $\pm e/2$ localized in one of the layers [1,2,5]. Because they are charged, merons can be nucleated by a disorder potential, and thus give rise to a correlation length ξ for the condensate phase, determined by the average distance between merons. Small domains of characteristic size ξ^2 act as individual JJs, well coupled to each other by counterflow currents. As the size of these domains varies randomly, averaging over it “washes away” the Fraunhofer diffraction pattern [9,17] and gives rise to a smooth decay of the tunneling current with the in-plane magnetic field [see Fig. 1(c) inset]. Based on this result one might expect that merons also destroy the Shapiro steps in QH bilayers. We address this question by studying the dynamics of a QH exciton condensate in the presence of microwave radiation. We find that Shapiro steps in the I - V characteristic are present at dc voltages

$$eV_{\text{dc}} = n\hbar\omega, \quad (n = 0, 1, 2, \dots), \quad (1)$$

despite the presence of the merons. Such steps were qualitatively anticipated in Ref. [7]. Here, we give a comprehensive description of the microwave response of exciton condensates by (i) quantitatively analyzing the dependence of Shapiro steps on microwave power, dissipation strength, and in-plane magnetic field, (ii) using a realistic parametrization to predict that Shapiro steps are experimentally observable despite the absence of a Fraunhofer pattern, (iii) showing that Josephson oscillations also result in resonant features in the microwave dynamical conductance, and lead to regions of absolute negative conductance

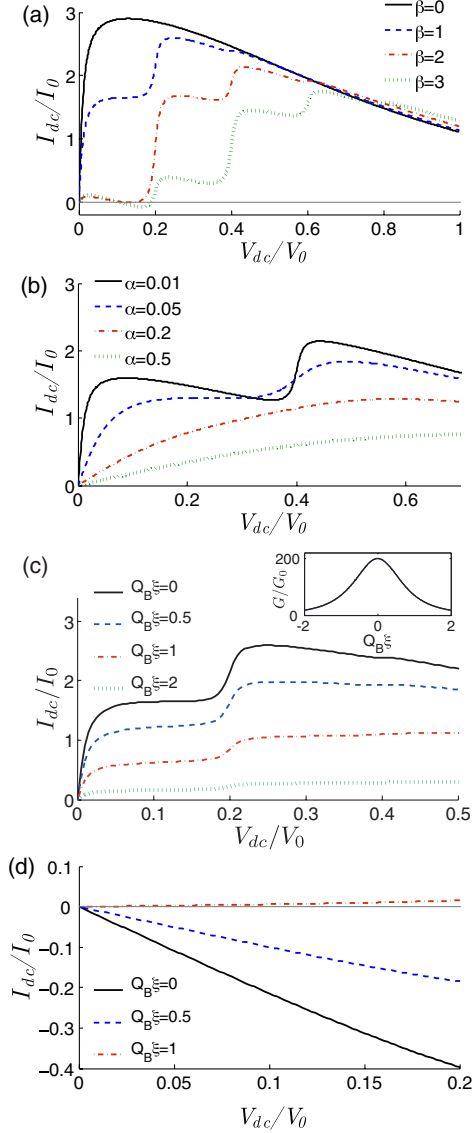


FIG. 1 (color online). (a) The I - V characteristics demonstrating Shapiro steps at voltages $eV_{dc} = n\hbar\omega$ ($n = 0, 1, 2, \dots$) for $\alpha = 0.01$, $\hbar\omega/eV_0 = 0.2$, $Q_B \equiv eB_{||}d/\hbar = 0$, and various $\beta \equiv eV_\omega/\hbar\omega$. (b) Dependence of the I - V characteristics on α for $\hbar\omega/eV_0 = 0.4$, $\beta = 1$, and $Q_B = 0$. For coherence times $\tau_\varphi = \alpha^{-1}\hbar/eV_0$ larger than $2\pi/\omega$, Shapiro steps are visible. (c) Suppression of Shapiro steps by an in-plane magnetic field $B_{||}$ for $\alpha = 0.01$, $\hbar\omega/eV_0 = 0.2$, and $\beta = 1$. Inset: Small-bias conductance $G = I_{dc}/V_{dc}$ as a function of $Q_B\xi$ for $\alpha = 0.01$ and $\beta = 0$ demonstrating the absence of the Fraunhofer pattern. Here, $G_0 = I_0/V_0$. (d) Demonstration of absolute negative conductance for $\alpha = 0.01$, $\hbar\omega/eV_0 = 0.3$, and $\beta = 2.4$. By increasing $B_{||}$, the direction of the current can be reversed. $I_{dc} = 0$ is marked with a thin gray line in (a) and (d).

(ANC), and (iv) discussing the fate of Shapiro steps in the regime of strong tunnel coupling.

We consider tunneling in the coherent phase at $\nu_T = 1$, and assume that the real spin is fully polarized. Then, the low-energy theory can be formulated in terms of a

pseudospin, which describes the *which layer* quantum degree of freedom and can also be considered as the exciton condensate order parameter [1,2,5]. The low-energy excitations of the system are the pseudospin waves and the merons. In the absence of tunneling, pseudospin waves are described by the Hamiltonian density [1,2,5,7]

$$\mathcal{H} = \frac{1}{2}\rho_s(\nabla\varphi)^2 + \frac{(en_0m_z/2)^2}{2\Gamma}, \quad (2)$$

where $\vec{m} = (\cos\varphi, \sin\varphi, m_z)$ is the pseudospin vector, ρ_s the pseudospin stiffness, Γ the capacitance per area and n_0 is the average density. The momentum conjugate to φ is $\pi = \hbar n_0 m_z/2$. The first term in Eq. (2) arises from the loss of Coulomb exchange energy if the pseudospin direction varies in space, and the second term measures the capacitive energy [5,7]. The dispersion relation of pseudospin waves described by the Hamiltonian (2) is $\omega_{\vec{k}} = uk$, with velocity $u = \sqrt{\rho_s e^2/\Gamma\hbar^2}$.

We consider a homogeneous time-dependent interlayer voltage $V(t)$. The tunneling energy and current operators are $H_T = T_+ + T_-$ and $\hat{I} = ie(T_+ - T_-)/\hbar$, where

$$T_{\pm}(t) = \frac{-\Delta_{SAS}}{8\pi l_B^2} e^{\pm ie \int_{t_0}^t V(t')dt'/\hbar} \int d^2r e^{\pm iQ_B x} e^{\pm i\varphi \pm i\varphi_m}.$$

Here Δ_{SAS} is the tunnel coupling between the two layers, $l_B = \sqrt{\hbar/eB}$ is the magnetic length, $Q_B = eB_{||}d/\hbar$, $B_{||}$ is the in-plane magnetic field, and d is the separation between the layers. Merons are included phenomenologically with the help of the vortex field φ_m [7,9,12]. Both counterflow and tunneling experiments suggest that fluctuations of φ_m are important. We characterize the vortex field fluctuations by a correlation length ξ and a correlation time τ_φ , such that $\langle e^{\pm i\varphi_m(\vec{r}_1, t_1)} e^{\mp i\varphi_m(\vec{r}_2, t_2)} \rangle = e^{-|\vec{r}_1 - \vec{r}_2|/\xi} e^{-|t_1 - t_2|/\tau_\varphi}$ and $\langle e^{\pm i\varphi_m(\vec{r}_1, t_1)} e^{\pm i\varphi_m(\vec{r}_2, t_2)} \rangle = 0$. These assumptions give rise to a quantitative agreement between theory and experiments; see Ref. [9].

Because of the vortex field fluctuations and small tunneling amplitude, tunneling acts as a bottleneck in charge transport, and the time-dependent tunneling current can be calculated perturbatively using linear response theory

$$I(t) = \frac{i}{\hbar} \int_{t_0}^t dt' \langle [H_T(t'), \hat{I}(t)] \rangle. \quad (3)$$

The solution for arbitrary time-dependent voltage

$$V(t) = V_{dc} + \sum_{k=1}^N V_{\omega_k} \cos(\omega_k t + \alpha_k) \quad (4)$$

can be computed by exploiting the relation

$$\langle e^{i\varphi(\vec{r}, t)} e^{-i\varphi(0,0)} \rangle = e^{1/2[\varphi(\vec{r}, t), \varphi(0,0)]} e^{-(1/2)\langle (\varphi(\vec{r}, t) - \varphi(0,0))^2 \rangle}.$$

In this way, we obtain

$$\begin{aligned}
I(t) = & \sum_{n_1, \dots, n_N} \sum_{m_1, \dots, m_N} \left[\prod_{k=1}^N J_{n_k}(\beta_k) J_{n_k+m_k}(\beta_k) \right] \\
& \times \left\{ I_S \left(eV_{\text{dc}} + \sum_{k=1}^N n_k \hbar \omega_k \right) \cos \left[\sum_{k=1}^N m_k (\omega_k t + \alpha_k) \right] \right. \\
& \left. + K_S \left(eV_{\text{dc}} + \sum_{k=1}^N n_k \hbar \omega_k \right) \sin \left[\sum_{k=1}^N m_k (\omega_k t + \alpha_k) \right] \right\}, \quad (5)
\end{aligned}$$

where $J_n(x)$ are Bessel functions, the summations are from $-\infty$ to ∞ and $\beta_k = eV_{\omega_k}/\hbar\omega_k$. Here, $I_S(eV_{\text{dc}}) = \text{Im}[F_S(eV_{\text{dc}})]$ is the static I - V characteristic in the absence of microwave field [7,9], and $K_S(eV_{\text{dc}}) = \text{Re}[F_S(eV_{\text{dc}})]$ is the real part of the complex function

$$\begin{aligned}
F_S(eV) = & \int dq \left[\frac{I_0}{q - eV/eV_0 - i\alpha} + \frac{I_0}{eV/eV_0 + q + i\alpha} \right] \\
& \times \int dR R e^{-R} J_0(qR) J_0(Q_B \xi R). \quad (6)
\end{aligned}$$

Here $q = k\xi$ and $R = r/\xi$ are momentum and radial coordinates, $I_0 = (e\xi^2 L^2 \Delta_{\text{SAS}}^2 e^{-D_0/2}) / (64\pi^2 \hbar \rho_s I_B^4)$ and $V_0 = \hbar u / e\xi$ determine the characteristic current and voltage scales, $\alpha(T) = \xi / u\tau_\varphi(T)$ is the temperature-dependent decoherence rate, $D_0 = \hbar u k_0 / (2\pi\rho_s)$, $k_0 = \kappa\sqrt{2}/l_B$ ($\kappa \approx 1$) is an ultraviolet cutoff momentum, and L^2 is the area of the sample. Because I_S and K_S are related to each other by the Kramers-Kronig relations, the response to an arbitrary ac field is completely determined by the static I - V characteristic.

The I - V characteristic obtained from Eq. (6) can be used to describe a large number of experimental observations [9]. In particular, by fitting $\xi \sim 100$ nm and $u \sim 14$ km/s, the smooth suppression of the conductance peak without the Fraunhofer oscillations and an appearance of the resonant enhancement of the tunneling current at $eV_{\text{dc}} = \hbar u Q_B$ in the presence of the in-plane magnetic field can be quantitatively described. Moreover, the temperature-dependent decoherence rate $\alpha(T)$ describes the height and width of the zero-bias conductance peak. The parameters V_0 and I_0 depend only weakly on temperature, and have typical values $V_0 \sim 100$ μ V and $I_0 \sim 5$ pA–1 nA [9]. The current scale I_0 can vary considerably, because the tunnel coupling Δ_{SAS} can be experimentally controlled over a wide range of values 10–100 μ K. For temperatures comparable to the thermal activation gap, the temperature dependence of α arises mainly due to thermally activated hopping of the merons. On the other hand, at smaller temperatures α shows a power-law-like temperature dependence, which could originate from low-energy excitation close the meron cores [10]. At the lowest experimental temperatures we obtain $\alpha \approx 0.01$ [9], which means that $\tau_\varphi \sim 1$ ns. Therefore we expect interesting features in the microwave response at GHz frequencies. In the

following we measure the frequency in scaled units as $\hbar\omega/eV_0$. A frequency $\omega/2\pi = 1$ GHz corresponds to $\hbar\omega/eV_0 \approx 0.04$.

Equation (5) for the time-dependent current, derived in this Letter for the bilayer exciton condensates, describes so-called Tucker relations, which have been considered earlier in various tunneling systems [30–34]. For slowly varying voltage, $\omega_i\tau_\varphi \ll 1$, the tunneling current follows the instantaneous value of the time-dependent voltage according to the static I - V characteristic $I(t) = I_S(eV(t))$, but for $\omega_i\tau_\varphi \gtrsim 1$ significant deviations from this relation can occur. We concentrate on the situation where the microwave field is monochromatic $V(t) = V_{\text{dc}} + V_\omega \cos\omega t$. In this case, the dc component I_{dc} and the ac components I_m^c, I_m^s of the time-dependent current can be written as

$$\begin{aligned}
I(t) = & I_{\text{dc}} + \sum_{m=1}^{\infty} [I_m^c \cos(m\omega t) + I_m^s \sin(m\omega t)], \\
I_{\text{dc}} = & \sum_n J_n^2(\beta) I_S(eV_{\text{dc}} + n\hbar\omega), \\
I_m^c = & \sum_n J_n(\beta) [J_{n+m}(\beta) + J_{n-m}(\beta)] I_S(eV_{\text{dc}} + n\hbar\omega), \\
I_m^s = & \sum_n J_n(\beta) [J_{n+m}(\beta) - J_{n-m}(\beta)] K_S(eV_{\text{dc}} + n\hbar\omega), \quad (7)
\end{aligned}$$

where the summations are from $-\infty$ to ∞ , and $\beta = eV_\omega/\hbar\omega$. Defining the dynamical conductance via $I_\omega = G(\omega)V_\omega$, we can identify $\text{Re}[G(\omega)] = I_1^c/V_\omega$, and $\text{Im}[G(\omega)] = -I_1^s/V_\omega$. Because all the microscopic parameters are known, we can use Eqs. (7) to calculate the microwave response of the QH exciton condensates. Our results for the I - V characteristics and dynamical conductance for different values of the dissipation strength, in-plane magnetic field, and the amplitude and frequency of the microwave field are shown in Figs. 1 and 2. Clear step-like structures appear in the I - V characteristic if $\hbar\omega/(2\pi eV_0) > \alpha$. Therefore for sufficiently low dissipation strength $\alpha = 0.01$, the Shapiro steps can be observed at GHz frequencies. As can be seen from Eqs. (7) and Figs. 1(a)–1(c), the Shapiro steps appear at voltages $eV_{\text{dc}} = n\hbar\omega$ ($n = 0, 1, 2, \dots$) and become sharper with decreasing dissipation strength α , so that in the limit $\alpha \rightarrow 0$, true steps appear in the I - V characteristic. The amplitude of the steps oscillates with the strength of the microwave power as can be seen from Eqs. (7). We find that at large microwave power, the current can become negative at positive voltage demonstrating ANC [Figs. 1(a) and 1(d)]. In particular, for microwave amplitudes around $\beta \approx 2.4$ [corresponding to $J_0(\beta) \approx 0$], the ANC occurs over a wide range of V_{dc} [Fig. 1(d)]. These features provide a clear signature of the ac Josephson effect, and their observation would help to unambiguously confirm the existence of an exciton condensate in $\nu_T = 1$ QH bilayers. Based on the above calculations, we conclude that Shapiro steps are a more robust experimental signature of the

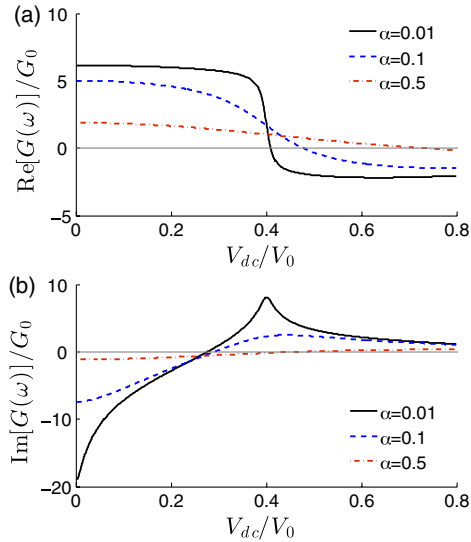


FIG. 2 (color online). (a) Real and (b) imaginary parts of the small signal dynamical conductance for $\hbar\omega/eV_0 = 0.4$ and different dissipation strengths α . The conductance is given in units $G_0 = I_0/V_0$. $\text{Re}[G(\omega)] = 0$ and $\text{Im}[G(\omega)] = 0$ are marked with a thin gray line.

Josephson effects than the Fraunhofer diffraction pattern, and they can also be observed in the presence of strong fluctuations of the vortex field.

We have also studied the dependence of the Shapiro steps and the ANC on the in-plane magnetic field. Once the magnetic field is strong enough to cause destructive quantum interference on the length scale ξ , the height of Shapiro steps is reduced [Fig. 1(c)], thus strengthening the interpretation of Shapiro steps as a consequence of quantum coherence. In the absence of microwaves, the in-plane magnetic field also gives rise to a resonance at voltage $eV_{dc} = \hbar\omega Q_B$ due to the Goldstone mode, so that one might expect to see resonant features at voltages $eV_{dc} = \hbar\omega Q_B + n\hbar\omega$. However, these wide resonances appear in a large range of voltages, and even in the absence of microwave radiation can be clearly observed only by studying the second derivative d^2I/dV^2 . On the other hand, we find that in the ANC parameter regime the wide resonances appearing in the static I - V characteristic in the presence of the in-plane field can be used to reverse the direction of the dc current [Fig. 1(d)].

In addition to Shapiro steps, characteristic resonant features also appear in the real and imaginary parts of the microwave dynamical conductance (see Fig. 2), calculated using Eqs. (7) for different values of the dissipation strength. As a function of V_{dc} , the real part of the dynamical conductance shows a dispersive profile around the resonance $eV_{dc} = \hbar\omega$, whereas the imaginary part shows a peak, when this condition is satisfied. Similarly as in the case of the I - V characteristic, for stronger amplitudes of the microwave field replicas of resonant features appear at voltages $eV_{dc} = n\hbar\omega$ ($n = 0, 1, 2, \dots$).

Finally, we compare the Shapiro steps and the resonant microwave response in exciton condensates to similar effects appearing in other tunneling systems. First, it is known that similar qualitative features, including resonant features in the I - V characteristic at $eV_{dc} = n\hbar\omega$, can occur in semiconductor heterostructures due to the photon-assisted tunneling [31–33]. However, important quantitative differences occur because the resonant features considered in this work appear due to the collective dynamics of the exciton condensate. Whereas the effects due to the photon-assisted transport can typically be seen in a THz frequency range [33], we predict that in QH exciton condensates the Shapiro steps exist already at GHz frequencies. Second, we would like to elaborate on the analogy to the Shapiro steps in JJs. For JJs it is possible to show rigorously that the I - V characteristic can be calculated using lowest order perturbation theory in the limit of large fluctuations, whereas the limit of vanishing fluctuations can be described by means of perturbation theory to all orders in the tunneling [35,36]. As a function of the decreasing temperature, the I - V characteristic develops from the perturbative limit with finite resistance smoothly to the usual Josephson supercurrent I - V characteristic with a critical current given by the Ambegaokar-Baratoff relation [35–37]. It is known that the microwave response in JJs in the presence of strong fluctuations is described by the Tucker relations [38], where the electron charge e is replaced by the Cooper pair charge $2e$. In particular, the Tucker relations predict that the heights of the Shapiro steps are proportional to $J_n^2(2eV_\omega/\hbar\omega)$. On the other hand, in ideal JJs the I - V characteristic is described by Werthamer relations [39,40], where the heights of the Shapiro steps are proportional to $J_n(2eV_\omega/\hbar\omega)$. Based on the analysis of the static I - V characteristic, one expects a smooth transition between these two regimes as a function of temperature. Our calculations in QH exciton condensates are in the experimentally relevant regime where Δ_{SAS} is small and the fluctuations of the vortex field are strong, so that the tunneling can be treated using the perturbation theory [9]. However, the parameter dependence of the critical tunnel current is the same as that found in a nonperturbative treatment of the strong tunneling regime [12]. Based on the analogy to JJs, we expect that if the temperature is decreased or Δ_{SAS} is increased, quantitative differences to our results will occur. However, similarly as in the case of JJs we may expect that the results obtained using the perturbation theory are qualitatively correct in all parameter regimes.

In summary, we have shown that microwave radiation gives rise to Shapiro steps in the I - V characteristic of QH bilayers, and we have predicted resonant features in the microwave dynamical conductance. According to our theoretical calculations, Shapiro steps are a more robust experimental signature of Josephson-like dynamics than the Fraunhofer diffraction pattern, because they do not depend on the spatial regularity of the condensate phase.

We would like to acknowledge valuable discussions with W. Dietsche, K. von Klitzing, J. Smet, X. Huang, D. Zhang, and K. N. Alekseev, and financial support by BMBF.

-
- [1] *Perspectives in Quantum Hall Effects*, edited by S. Das Sarma and A. Pinczuk (Wiley, New York, 1997).
- [2] S. M. Girvin, in *The Quantum Hall Effect: Novel Excitations and Broken Symmetries*, edited by A. Comtet, T. Jolicœur, S. Ouvry, and F. David Proceedings of the Les Houches Summer School (Springer-Verlag, Berlin, 1999).
- [3] J. P. Eisenstein and A. H. MacDonald, *Nature (London)* **432**, 691 (2004).
- [4] H. A. Fertig, *Phys. Rev. B* **40**, 1087 (1989).
- [5] K. Moon, H. Mori, K. Yang, S. M. Girvin, A. H. MacDonald, L. Zheng, D. Yoshioka, and S.-C. Zhang, *Phys. Rev. B* **51**, 5138 (1995).
- [6] X. G. Wen and A. Zee, *Phys. Rev. B* **47**, 2265 (1993); Z. F. Ezawa and A. Iwazaki, *Phys. Rev. B* **47**, 7295 (1993); *Int. J. Mod. Phys. B* **08**, 2111 (1994).
- [7] A. Stern, S. M. Girvin, A. H. MacDonald, and N. Ma, *Phys. Rev. Lett.* **86**, 1829 (2001).
- [8] L. Balents and L. Radzihovsky, *Phys. Rev. Lett.* **86**, 1825 (2001); M. M. Fogler and F. Wilczek, *Phys. Rev. Lett.* **86**, 1833 (2001).
- [9] T. Hyart and B. Rosenow, *Phys. Rev. B* **83**, 155315 (2011).
- [10] H. A. Fertig and J. P. Straley, *Phys. Rev. Lett.* **91**, 046806 (2003); H. A. Fertig and G. Murthy, *Phys. Rev. Lett.* **95**, 156802 (2005).
- [11] P. R. Eastham, N. R. Cooper, and D. K. K. Lee, *Phys. Rev. B* **80**, 045302 (2009).
- [12] P. R. Eastham, N. R. Cooper, and D. K. K. Lee, *Phys. Rev. Lett.* **105**, 236805 (2010).
- [13] J.-J. Su and A. H. MacDonald, *Phys. Rev. B* **81**, 184523 (2010).
- [14] I. B. Spielman, J. P. Eisenstein, L. N. Pfeiffer, and K. W. West, *Phys. Rev. Lett.* **84**, 5808 (2000).
- [15] I. B. Spielman, J. P. Eisenstein, L. N. Pfeiffer, and K. W. West, *Phys. Rev. Lett.* **87**, 036803 (2001).
- [16] M. Kellogg, I. B. Spielman, J. P. Eisenstein, L. N. Pfeiffer, and K. W. West, *Phys. Rev. Lett.* **88**, 126804 (2002).
- [17] I. B. Spielman, Ph.D. thesis, Caltech, 2004.
- [18] M. Kellogg, J. P. Eisenstein, L. N. Pfeiffer, and K. W. West, *Phys. Rev. Lett.* **93**, 036801 (2004); E. Tutuc, M. Shayegan, and D. A. Huse, *Phys. Rev. Lett.* **93**, 036802 (2004).
- [19] R. D. Wiersma, J. G. S. Lok, S. Kraus, W. Dietsche, K. von Klitzing, D. Schuh, M. Bichler, H.-P. Tranitz, and W. Wegscheider, *Phys. Rev. Lett.* **93**, 266805 (2004).
- [20] A. D. K. Finck, A. R. Champagne, J. P. Eisenstein, L. N. Pfeiffer, and K. W. West, *Phys. Rev. B* **78**, 075302 (2008).
- [21] L. Tiemann, Y. Yoon, W. Dietsche, K. von Klitzing, and W. Wegscheider, *Phys. Rev. B* **80**, 165120 (2009).
- [22] Y. Yoon, L. Tiemann, S. Schmult, W. Dietsche, and K. von Klitzing, *Phys. Rev. Lett.* **104**, 116802 (2010).
- [23] A. D. K. Finck, J. P. Eisenstein, L. N. Pfeiffer, and K. W. West, *Phys. Rev. Lett.* **106**, 236807 (2011).
- [24] X. Huang, W. Dietsche, M. Hauser, and K. von Klitzing, *Phys. Rev. Lett.* **109**, 156802 (2012).
- [25] H. Min, R. Bistritzer, J.-J. Su, and A. H. MacDonald, *Phys. Rev. B* **78**, 121401(R) (2008); Y. E. Lozovik and A. A. Sokolik, *JETP Lett.* **87**, 55 (2008); C.-H. Zhang, and Y. N. Joglekar, *Phys. Rev. B* **77**, 233405 (2008).
- [26] B. Seradjeh, H. Weber, and M. Franz, *Phys. Rev. Lett.* **101**, 246404 (2008).
- [27] B. Seradjeh, J. E. Moore, and M. Franz, *Phys. Rev. Lett.* **103**, 066402 (2009).
- [28] J. M. Rowell, *Phys. Rev. Lett.* **11**, 200 (1963).
- [29] S. Shapiro, *Phys. Rev. Lett.* **11**, 80 (1963).
- [30] J. R. Tucker, *IEEE J. Quantum Electron.* **15**, 1234 (1979); J. R. Tucker and M. J. Feldman, *Rev. Mod. Phys.* **57**, 1055 (1985).
- [31] A. Wacker, *Phys. Rep.* **357**, 1 (2002).
- [32] G. Platero and R. Aguado, *Phys. Rep.* **395**, 1 (2004).
- [33] B. J. Keay, S. Zeuner, S. Allen, K. Maranowski, A. Gossard, U. Bhattacharya, and M. Rodwell, *Phys. Rev. Lett.* **75**, 4102 (1995); S. Zeuner, B. Keay, S. Allen, K. Maranowski, A. Gossard, U. Bhattacharya, and M. Rodwell, *Phys. Rev. B* **53**, R1717 (1996).
- [34] G. Falci, V. Bubanja, and G. Schön, *Z. Phys. B* **85**, 451 (1991); Y. Koval, M. V. Fistul, and A. V. Ustinov, *Phys. Rev. Lett.* **93**, 087004 (2004).
- [35] G.-L. Ingold, H. Grabert, and U. Eberhardt, *Phys. Rev. B* **50**, 395 (1994); H. Grabert, G.-L. Ingold, and B. Paul, *Europhys. Lett.* **44**, 360 (1998).
- [36] Y. M. Ivanchenko and L. A. Zil'berman, *Sov. Phys. JETP* **28**, 1272 (1969); V. Ambegaokar and B. I. Halperin, *Phys. Rev. Lett.* **22**, 1364 (1969).
- [37] A. Steinbach, P. Joyez, A. Cottet, D. Esteve, M. Devoret, M. Huber, and J. Martinis, *Phys. Rev. Lett.* **87**, 137003 (2001).
- [38] The Tucker relation for I_{dc} in Eqs. (7) has been derived in Ref. [34], but the full set of Tucker relations can also be derived for JJs in the presence of strong fluctuations: T. Hyart and K. N. Alekseev (unpublished).
- [39] N. R. Werthamer, *Phys. Rev.* **147**, 255 (1966).
- [40] C. A. Hamilton, *Phys. Rev. B* **5**, 912 (1972).